Single Ion Mass Spectrometry at 100 ppt and Beyond

S. Rainville, J.K. Thompson, and D.E. Pritchard

Research Laboratory of Electronics, Department of Physics, Massachusetts Institute of Technology, Cambridge, MA 02139, U.S.A.

Abstract. Using a Penning trap single ion mass spectrometer, our group has measured the atomic masses of 14 isotopes with a fractional accuracy of about 10^{-10}. The masses were extracted from 28 cyclotron frequency ratios of two ions altenately confined in our trap. The precision on these measurements was limited by the temporal fluctuations of our magnetic field during the 5–10 minutes required to switch from one ion to the other. By trapping two different ions in the same Penning trap at the same time, we can now simultaneously measure their two cyclotron frequencies and extract the ratio with a precision of about 10^{-11} in only a few hours. We have developed novel techniques to measure and control the motion of the two ions in the trap and we are currently using these tools to carefully investigate the important question of systematic errors in those measurements.

1 Overview

Accuracy in mass spectrometry has been advanced over two orders of magnitude by the use of resonance techniques to compare the cyclotron frequencies of single trapped ions. This paper provides an overview of the MIT Penning trap apparatus, techniques and measurements. We begin by describing the various interesting applications of our mass measurements and the wide-ranging impact they have on both fundamental physics and metrology. In the same section, we also describe further scientific applications that an improved accuracy would open. This serves as a motivation for our most current work (described in Sect. 4) to increase our precision by about an order of magnitude.

Before describing the latest results, we give in Sect. 3 an overview of our apparatus and methods, with special emphasis on the techniques which we have developed for making measurements with accuracy around 10^{-10}. In those measurements, we alternately trapped two different ions (one at the time) and compared their cyclotron frequencies to obtain their mass ratio. The main limitation of this method was the fact that our stable magnetic field would typically fluctuate by several parts in 10^{10} during the 5–10 minutes required to switch from one ion to the other. In order to eliminate this problem, we now confine both ions simultaneously in our Penning trap. In Sect. 4, we describe the various techniques that have allowed us to load a pair in the trap and demonstrate a significant gain in precision from simultaneously measuring both their cyclotron frequencies. New tools to measure and control the motion of the ions are also presented. Those tools are invaluable in our current investigation of the important question

S.G. Karshenboim, V.B. Smirnov (Eds.): LNP 627, pp. 177–197, 2003.

of systematic errors. Unfortunately, because this work is ongoing at the time of this publication, we cannot report a new mass ratio measurement, but this new technique shows promise to expand the precision of mass spectrometry an order of magnitude beyond the current state-of-the-art. Finally, we discuss in Sect. 5 two other techniques that will address the next source of random error in our measurements: cyclotron amplitude fluctuations. Both techniques (squeezing and electronic refrigeration) have already been demonstrated by our group.

It should be noted that in addition to our work in ultra-high precision mass spectrometry, R. Van Dyck's group at the University of Washington has performed measurements of 7 atomic species and their results for the same ions agree satisfactorily with our masses [1–3].

2 Scientific Applications

Of the three basic physical quantities – mass, length, and time – mass is currently measurable with the least accuracy. This is unfortunate because mass uncertainties are often the limiting factor in precision experiments and metrology. Also, accurate mass differences between initial and final states directly determine the energy available for a variety of interesting physical and chemical processes (e.g. emission of a gamma ray, neutrino, neutron, or electron, and chemical reactions).

To date we have measured a total of 14 neutral masses, ranging from the masses of the proton and neutron to the mass of ^{133}Cs, all with accuracies near or below 10^{-10} – one to three orders of magnitude better than the previously accepted values [4,5]. Our mass measurements have wide-ranging impact on both fundamental physics and metrology. The masses of hydrogen and of the neutron are considered fundamental constants [6]. The neutron capture processes ^{12}C(n,γ) and ^{14}N(n,γ) emit gamma rays used as calibration lines in the 2–10 MeV range of the gamma spectrum; our measurement of ^{15}N-^{14}N revealed an 80 eV error (8 times the quoted error) in the most widely used standard and lowered its error to 1 eV [4]. Our ^{20}Ne measurement resolved a huge discrepancy (reflected in the old error) involving determination of atomic masses from the energy of nuclear decay products. Also, our result for the mass of ^{28}Si is necessary for one scheme to replace the artifact kilogram (the only non-physics based metrological standard) by defining Avogadro's number.

Finally our most recent mass measurements of the four alkali atoms ^{133}Cs, ^{87}Rb, ^{85}Rb and ^{23}Na have opened a new route to the fine structure constant α [5]. Indeed, a route to α that appears likely to yield a value at the ppb level is obtained by expressing the fine structure constant in terms of experimentally measurable quantities as follows (in SI units):

$$\alpha^2 = 2cR_\infty \frac{f_{\rm rec}}{f_{D1}^2} \frac{M_{\rm Cs}}{M_{\rm e}}. \tag{1}$$

The Rydberg constant R_∞ has been measured to an accuracy of 0.008 ppb [7], the frequency of the cesium D1-line $f_{\rm D1}$ was measured by Hänsch's group at the Max-Planck-Institut in Garching to 0.12 ppb [8], and the mass of the electron

in atomic mass units M_e was recently obtained to 0.8 ppb from a measurement of the g factor of the bound electron in $^{12}C^{5+}$ [9] (in reasonable agreement with the previous value at 2 ppb from VanDyck's group [10]). The mass of ^{133}Cs in atomic mass units M_{Cs} was previously known to 23 ppb and we measured it to 0.2 ppb. Finally, the recoil frequency shift f_{rec} of a Cs atom absorbing photons of laser light at the D_1 line is being measured in Chu's group at Stanford University. There has been recent reports of a value of f_{rec} at or below 10 ppb but it has not been published yet. Combining these results in (1) will lead to a new determination of α with a precision of about 5 ppb. This is similar to the precision of the current best measurement of alpha from the $g-2$ factor of the electron combined with QED calculations (4 ppb) and can therefore be regarded as a check of QED at an unprecedented level of precision. In addition to resting on such simple and solid physical foundations, this route has the advantage that it can be exploited with many different atomic systems. An experiment is already under way at the Laboratoire Kastler Brossel (ENS, France) to measure the atomic recoil frequency shift in Rb [11] and a new type of interferometer has been demonstrated at MIT (USA) to measure the same quantity in Na [12].

Another interesting application for precise mass measurements involves measuring the mass difference between two atoms related by a neutron capture process, like ^{15}N and ^{14}N. Kessler and collaborators at NIST have precisely measured the wavelengths of the γ-rays emitted in a few neutron capture processes [13]. By comparing the energy of the γ-rays to the mass difference between the initial and final states, one can look for a violation of special relativity. The basic idea is to write

$$\Delta m c_m^2 = \frac{h c_{em}}{\lambda} \tag{2}$$

in which a photon of wavelength λ is emitted in a process where a mass Δm is converted into electromagnetic radiation. The quantities c_m and c_{em} are respectively defined as the limiting velocity of a massive particle and the velocity of propagation of an electromagnetic wave in vacuum. According to the special theory of relativity, these two quantities are the same, i.e., $c_m = c_{em}$. Independent measurements of λ and Δm could ultimately place limits on the quantity $(1 - c_m/c_{em})$ at the level of $(1 \text{ to } 2)\times 10^{-7}$. This would improve the current limit (from the Compton wavelength of the electron and the von Klitzing constant) by about two orders of magnitude [14]. Unlike other tests of special relativity (Michelson-Morley, Kennedy-Thorndike, etc.), this limit does not depend on assumptions concerning the motion of the laboratory with respect to a preferred reference frame. In order to determine Δm with the same precision as the one reached by the NIST group on λ (few parts in 10^7), we need to be able to make mass comparisons with an accuracy of a few parts in 10^{11}.

Mass being such a fundamental quantity of matter (and one of the three basic physical quantities), it is inevitable that measuring it more precisely will open new possibilities in metrology and challenge our understanding of nature. More specifically, in addition to the application mentioned above, new mass measurements with a precision of 10^{-11} could provide new metrological benchmarks and help determine the mass of the electron neutrino (with the $^3H-^3He$ mass dif-

ference) [15,16]. If we could reach our ultimate goal of 10^{-12}, we would have a generally useful technique to directly measure excitation and chemical binding energies of atomic and molecular ions by weighing the associated small decrease in mass, $\Delta E = \Delta m c^2$. A novel technique we have recently developed that shows promise towards achieving those goals will be discussed in Sect. 4.

3 Experimental Techniques

Our atomic masses are determined by comparing the cyclotron frequencies $\omega_c = qB/m$ of single atomic or molecular ions. The ions are held in a Penning trap which consists of a strong uniform magnetic field (8.5 T) and a weak dc quadrupole electric field to confine the ions along the direction of the magnetic field. The electric field is generated by a set of hyperbolic electrodes shown on Fig. 2. Another set of electrodes, called guard rings, are located on the hyperbolic assymptotes and are adjusted to approximately half the voltage on the ring electrode in order to minimize the lowest order non-quadrupole electric field component (C_4). The electrode surfaces are coated with graphite (Aerodag) to minimize charge patches. Together with the magnetic field, they form what is called an orthogonally compensated hyperbolic Penning trap with characteristic size $d = 0.549\,\mathrm{cm}$. At rf frequencies, the guard rings are split in order to provide dipole drives and quadrupole mode couplings for the radial modes (see Sect. 3.2). Figure 1 shows the location of the Penning trap relative to the rest of our apparatus. Trapping the ion allows the long observation time necessary for high precision. Using a single ion is crucial for high accuracy since this avoids the frequency perturbations caused by the Coulomb interaction between multiple ions.

The combination of magnetic and electric fields in our Penning trap results in three normal modes of motion: trap cyclotron, axial, and magnetron, with frequencies $\omega_c'/2\pi \approx 5\,\mathrm{MHz} \gg \omega_z/2\pi \approx 0.2\,\mathrm{MHz} \gg \omega_m/2\pi \approx 0.005\,\mathrm{MHz}$, respectively. The free-space cyclotron frequency ω_c is recovered from the quadrature sum of the three normal mode frequencies (invariant with respect to trap tilts and ellipticity [17]):

$$\omega_c = \frac{qB}{m} = \sqrt{\omega_{c'}^2 + \omega_z^2 + \omega_m^2}\,. \tag{3}$$

We produce ions by ionizing neutral gas in our trap. From a room temperature gas-handling manifold we inject a small amount of neutral gas at the top of our apparatus (Fig. 1) and it diffuses down into the trap through a small hole in the upper endcap. From a field emission tip at the bottom of the trap (shown on Fig. 2), we generate a very thin electron beam (sub-μm diameter) which then ionizes atoms or molecules inside the trap. Since the electron beam is parallel and close to the trap axis, the ions are created with a small magnetron radius ($\leq 100\,\mu\mathrm{m}$). We test for the presence of ions by applying a short drive pulse on the lower end cap and looking for the ions' signal in our detector (see Sect. 3.1). We determine the number of (identical) ions produced by measuring the damping time of the ion signal. If more than two ions are present, we normally invert

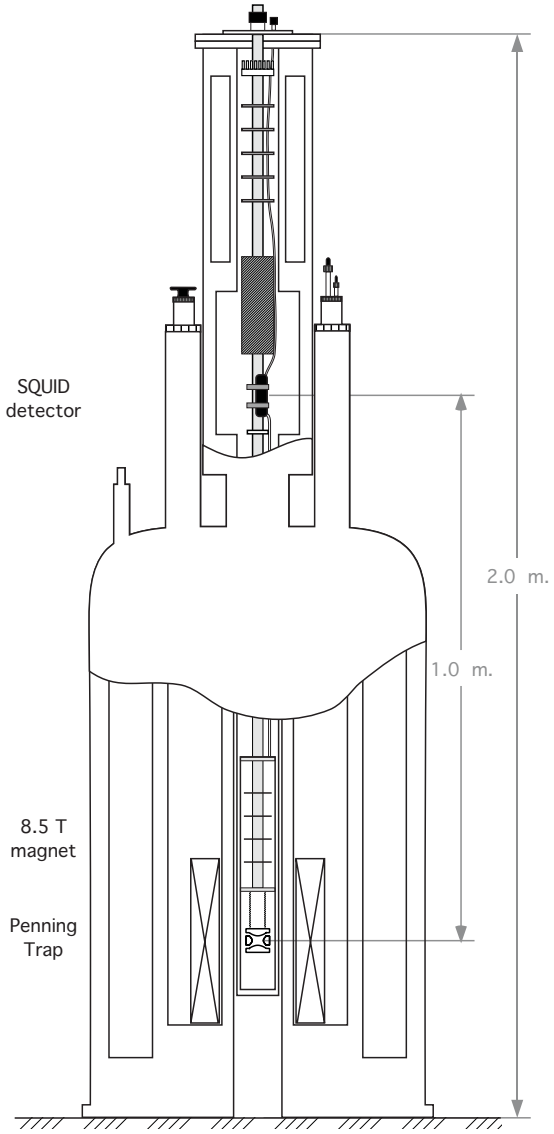

Fig. 1. Schematic of the ion mass spectrometer at MIT. The superconducting magnet produces a stable 8.5 T magnetic field. The image current induced in the endcap by the ion's axial motion is detected using a dc SQUID. The trap, the magnet and the SQUID are at liquid helium temperature (4 K)

the trap and try again. We gradually reduce the amount of gas used, the electron beam current and the time we leave it on until we make, on average, a single ion of the kind we want. Since this ion making procedure is not selective, it sometimes produces unwanted ions with different masses. For example, if we use N_2 gas to make one N_2^+ ion, we might also make N^+ ion(s). We eliminate these so called "fragments" by selectively exciting their axial motion (since they have a different mass/charge ratio, their axial frequency is different) and then bringing the equilibrium position of the ion cloud very near the lower endcap (by applying

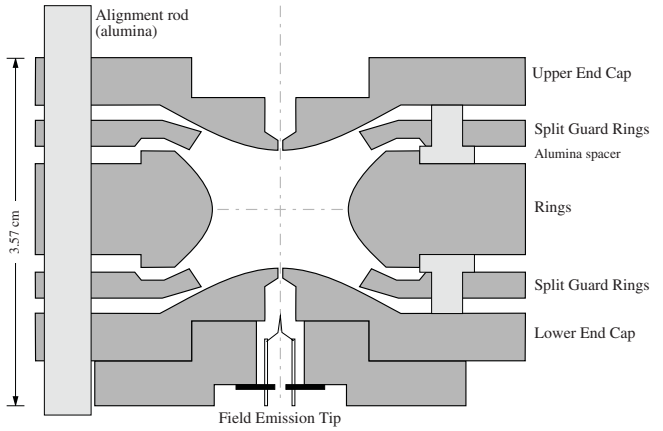

Fig. 2. Cross section of our orthogonally compensated hyperbolic Penning Trap. The copper electrodes are hyperbolae of rotation and form the equipotentials of a weak quadrupole electric field. Guard ring electrodes located on the hyperbolic assymptotes are adjusted to minimize the lowest order non-quadrupole electric field component. The electrode surfaces are covered with a thin layer of graphite (Aerodag) to minimize charge patches

a dc voltage to it). The highly excited ions then neutralize by striking the encap and we are left with only the desired ion in the trap. If 2 or 3 identical ions remain in the trap, bringing them progressively closer and closer to the endcap has a good chance of thining the cloud down to only a single one.

3.1 SQUID Detector

We have developed ultrasensitive superconducting electronics to detect the miniscule currents ($\leq 10^{-14}$ amperes) that a single ion's axial motion induces in the trap electrodes. The detector consists of a dc SQUID coupled to a hand wound niobium superconducting resonant transformer ($Q \approx 45\,000$) connected across the endcaps of the Penning trap [18]. Our detection noise is currently dominated by the 4 K Johnson noise present in the resonant transformer – a fact we have exploited as discussed in Sect. 5.2. Energy loss in the resonant transformer damps the axial motion on a time scale of typically 1 second (at $m/q \approx 30$), quickly bringing the axial motion to thermodynamic equilibrium at 4 K. Since the ion signal is concentrated in a narrow frequency band, we can easily detect it against the broad Johnson noise with a signal-to-noise ratio of about 10.

Due to the superconducting nature of our detector, both the SQUID and the transformer have to be located about 1 m away from the trap in a region of relatively low the magnetic field (see Fig. 1). They are both encased in separate superconducting niobium boxes wrapped with lead. When the apparatus is cooled down, external bucking coils zero the magnetic field at the location of the detector. Once the niobium boxes are superconducting, they keep magnetic flux

out and allow the operation of the detector without any current in the bucking coils.

3.2 Mode Coupling and π-Pulses

The axial oscillation frequency of any ion can be tuned into resonance with the fixed detector frequency by changing the dc trapping voltage. To be able to measure the cyclotron frequency using only our axial mode detector, we use a resonant rf quadrupole electric field which couples the cyclotron and axial modes [19]. This coupling causes the two modes to cyclically and phase coherently exchange their classical actions (amplitude squared times frequency). In analogy to the Rabi problem, a π-pulse can be created by applying the coupling just long enough to cause the coupled modes to exactly exchange their actions. The same rf quadrupole field is also used to cool the cyclotron mode by coupling it continuously to the damped axial mode. By using a different rf frequency, the exact same technique can be used to measure and cool the magnetron mode.

3.3 Pulse and Phase Technique

We have developed the Pulse aNd Phase (abbreviated PNP) method to achieve a relative uncertainty of 10^{-10} on cyclotron frequency measurements in less than 1 minute [20]. A PNP measurement starts by cooling the trap cyclotron mode via coupling to the damped axial mode (see Sect. 3.2). The trap cyclotron motion is then driven to a reproducible amplitude and phase at $t = 0$ and then allowed to accumulate phase for some time T, after which a π-pulse is applied. The phase of the axial signal immediately after the π-pulse is then measured with rms uncertainty of order 10 degrees. Because of the phase coherent nature of the coupling, this determines the cyclotron phase with the same uncertainty. The trap cyclotron frequency is determined by measuring the accumulated phase versus evolution time T with the shorter times allowing the measured phase (which is modulo 360 degrees) to be properly unwrapped. Since we can typically measure the phase within 10 degrees, a cyclotron phase evolution time of about 1 minute leads to a determination of the cyclotron frequency with a precision of 10^{-10}.

The PNP method has the advantage of leaving the ion's motion completely unperturbed during the cyclotron phase evolution [19]. It is also particularly suited to measure mass doublets – pairs of species such as CD_4^+ and Ne^+ that have the same total atomic number. Good mass doublets typically have relative mass difference of less than 10^{-3}, making these comparisons insensitive to many systematic instrumental effects.

3.4 Separate Oscillatory Field Technique

To compare an ion to ^{12}C, it is crucial to determine the masses of ^1H and D (^2H) so that they can be combined with ^{12}C to form doublet comparison molecules (for instance O^+/CH_4^+ and Ne^+/CD_4^+) since comparing near equal

masses reduces the size of many experimental systematic errors. Therefore, it is crucial to determine the masses of ^{1}H and D. However, there are very few routes for doing this with doublet comparisons and even fewer direct routes involving a single mass doublet comparison.

To illustrate why it is difficult to find a series of doublet mass ratios which yield masses of ^{1}H and D, consider the set of comparisons (i.e. mass ratios)

$$\frac{\mathrm{N}^+}{\mathrm{CH}_2^+}\ ,\ \frac{\mathrm{O}^+}{\mathrm{CH}_4^+}\ ,\ \frac{\mathrm{CO}^+}{\mathrm{N}_2^+}$$

which would seem to determine the three unknown atomic masses H, N and O (i.e. relative to C). A doublet mass ratio is so close to 1 that it should be thought of as determining a mass difference. For example, if $R \equiv \mathrm{N}^+/\mathrm{CH}_2^+$ then

$$\mathrm{N}^+ - \mathrm{CH}_2^+ \approx (R-1)(\mathrm{CH}_2^+)' = \Delta M < 0.001 \times (\mathrm{CH}_2^+)'$$

where the mass $(\mathrm{CH}_2^+)'$ is known from other experiments with several orders of magnitude less accuracy. From this perspective and after correcting for ionization and molecular binding energies, the above set of measured cyclotron frequency ratios determine the mass differences

$$\begin{aligned}
\mathrm{N} - \mathrm{C} - 2\mathrm{H} &= \Delta M_1\ , \\
\mathrm{O} - \mathrm{C} - 4\mathrm{H} &= \Delta M_2\ , \\
\mathrm{O} + \mathrm{C} - 2\mathrm{N} &= \Delta M_3\ .
\end{aligned}$$

Unfortunately, it is clear that these relations yield only 2 linearly independent equations– combining the first two equations yields the third which therefore is a consistency check on the three measurements. Using non-doublet ratios such as $\mathrm{CD}_4^+/\mathrm{C}^+$ and $\mathrm{CH}_4^+/\mathrm{C}^+$ removes such singularities from the matrix relating neutral atomic masses to measured mass differences.

In the case of a non-doublet comparison, the difference in the trapping voltages needed to detect each ion's axial motion is large enough to cause significant shifts in the ion's equilibrium position due to charge patches on the trap electrodes. The shift in equilibrium position causes a systematic error because of magnetic field inhomogeneities.

We have developed the SOF (separated oscillatory field) technique [21] to allow us to make cyclotron frequency comparisons using the same trapping voltage during the phase evolution time. An SOF sequence is identical to the PNP sequence but with a second drive pulse equal in strength to the first in place of the π-pulse. If the second drive pulse is in (out of) phase with the cyclotron motion, the two drive pulses add (subtract) resulting in a large (small) cyclotron amplitude. The result is that the cyclotron's phase information is encoded in the cyclotron amplitude. The trapping voltages can be adiabatically adjusted for axial detection and a π-pulse then applied. The detected axial amplitude versus phase evolution time T produces a classical Ramsey fringe which oscillates at the difference between the drive and trap cyclotron frequencies.

3.5 Making a Mass Table

A cyclotron frequency ratio of two different ions is determined by a run measuring a cluster of ω_c values for an ion of type A, then for type B, etc. In a typical 4-hour run period (from 1:30-5:30 am when the nearby electrically-powered subway is not running), we can typically record between 5 and 10 alternations of ion type (see Fig. 3).

Since the measured free-space cyclotron frequencies exhibit a common slow drift, we fit a polynomial plus a frequency difference to the combined set of cyclotron frequency measurements for the night. The average polynomial fit order is typically between 3 and 5 and is chosen using the F-test criterion [22] as a guide to avoid removing frequency changes which are not correlated between ion types. The distribution of residuals from the polynomial fits has a Gaussian center with a standard deviation $\sigma_{\text{resid}} \approx 0.25$ ppb and a background ($\approx 2\,\%$ of the points) of non-Gaussian outliers [4]. We handle these non-Gaussian outliers using a robust statistical method to first properly describe the observed statistical distribution of data points and then to smoothly deweight the nongaussian points [23,4].

In all, we have measured a set of 28 cyclotron frequency ratios during 55 night runs using the techniques described above. In order to convert those ion mass ratios to mass differences of neutral isolated atoms, we account for chemical binding energies and for the mass of the missing electrons and their ionization energies [24,25]. Because those are small corrections and they are known with enough precision, they don't contribute to our final uncertainties. Performing a global least square fit to all these linear equations yields the neutral atomic masses in Table 1. The fit produces a covariance matrix which directly yields the uncertainty in the atomic mass and allows uncertainties to be calculated for quantities involving correlated isotopes. Atomic masses are expressed relative

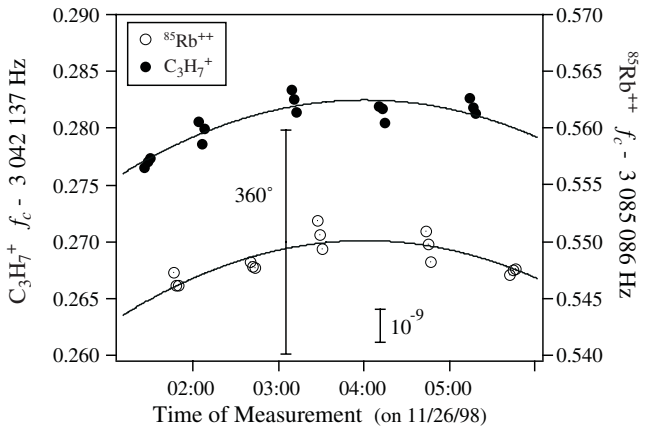

Fig. 3. Typical set of data comparing the cyclotron frequencies of two single ions alternately loaded into the Penning Trap. Magnetic field drifts (fitted here with a polynomial) limit the relative precision on the mass ratio to about 10^{-10}

Table 1. Neutral masses measured at MIT

Species	MIT Mass (u)	ppb	$\frac{\sigma_{1983}}{\sigma_{MIT}}$
^{1}H	1.007 825 031 6 (5)	0.50	24
n	1.008 664 916 4 (8)	0.81	17
^{2}H	2.014 101 777 9 (5)	0.25	48
^{13}C	13.003 354 838 1 (10)	0.08	17
^{14}N	14.003 074 004 0 (12)	0.09	22
^{15}N	15.000 108 897 7 (11)	0.07	36
^{16}O	15.994 914 619 5 (21)	0.13	24
^{20}Ne	19.992 440 175 4 (23)	0.12	957
^{23}Na	22.989 769 280 7 (28)	0.12	93
^{28}Si	27.976 926 532 4 (20)	0.07	350
^{40}Ar	39.962 383 122 (33)	0.08	424
^{85}Rb	84.911 789 732 (14)	0.16	193
^{87}Rb	86.909 180 520 (15)	0.17	187
^{133}Cs	132.905 451 931 (27)	0.20	111

to ^{12}C, which is defined to have a mass of exactly 12 atomic mass units (u). In Table 1, the error in the last digits is in parenthesis. The last two columns give the fractional accuracy of the measurements in ppb (parts in 10^9) and the improvement in accuracy over pre-Penning Trap mass values (from the 1983 atomic mass evaluation [26]). Note that the mass of the neutron is determined from the masses of ^{1}H and ^{2}H combined with measurements of the deuteron binding energy which has recently been improved [27].

The measured ratios were chosen so that at least two completely independent sets of mass ratios enter into the determination of each atomic mass. The overall $\chi^2_\nu = 0.83$, indicating excellent internal consistency. Other experimental checks on systematic errors include measuring calculable mass to charge ratios (i.e. $Ar^{++}/\ Ar^{+}$) and measuring redundant mass ratios at different mass to charge ratios which would have very different systematic errors (i.e. O^+/CH_4^+, $CO^+/C_2H_4^+$, and $CO_2^+/C_3H_8^+$ all determine the same mass difference C + 4H - O at $m/q = 16$, 28, and 44).

Regarding the important question of systematic errors, our group has been in a somewhat unique situation for precision experiments. All the possible systematic errors were estimated (and some of them experimentally tested) to be

well below the level of the random errors introduced by our magnetic field fluctuations. In other words, the errors on our measurements are entirely dominated by statistical noise from the magnetic field. The various self-consistency checks mentioned above confirmed that this is really the case and no unknown systematic errors are lurking at the level of our errors. The only exception to this situation was in the measured ratios involving Cs and Rb (the heaviest elements in our mass table). When repeatedly measuring those mass ratios for several nights, we found variations larger than our estimated error bar for each night ($\chi^2_\nu \approx 5$). Despite extensive research, we never identified the source of those excess night-to-night variations and we increased the error bars of our reported results to account for those fluctuations (see [5] for more details).

4 Simultaneous Measurements

Until the year 2000, we determined mass ratios by alternately creating individual ions of the two species being compared and measuring their cyclotron frequencies separately as described in the previous section. The precision of this technique is limited almost entirely by temporal fluctuations of the magnetic field, which are typically 3 parts in 10^{-10} during the several minutes required to trap a new single ion. We were also restricted to take precision cyclotron frequency measurements only during the period between about 01:00 and 05:30 at night during which Boston's electric subway is not running (it creates random fluctuations of about 4×10^{-7} T in our lab). In the fall of the year 2000, to avoid the effect of magnetic field fluctuations, we decided to make *simultaneous* measurements of the cyclotron frequencies of the two ions being compared.

Simultaneously comparing the cyclotron frequencies of two different ions in the same trap offers the best protection against magnetic field fluctuations and field gradients, but introduces new complications: ion-ion perturbations and systematic shifts due to spatial field inhomogeneities. In previous work studying the classical, two-body problem of two ions in a single Penning trap [28], we found that if we keep the distance between the ions large enough, the several kHz difference between the two ions' cyclotron frequencies keeps the two cyclotron modes independent from each other. Similarly, the axial frequencies of the two ions are different enough ($\Delta f_z \approx 50$ Hz) to keep the two axial modes uncoupled.

In contrast, since ω_m is to first order independent of mass, the Coulomb interaction between the ions couples the nearly frequency-degenerate magnetron modes into two new collective magnetron modes: a center-of-mass (COM) mode and a difference mode [28]. The COM mode corresponds to the center-of-mass of the ions moving at the average magnetron frequency (~ 5 kHz) about the center of the trap. The difference mode corresponds to an $E \times B$ drift of the ions about the center-of-mass due to the Coulomb interaction between them. The frequency of the difference mode is ~ 50 mHz higher than that of the COM mode. In [28], we showed that in a perfect trap the ion-ion separation distance ρ_s, i.e., the amplitude of the difference mode is constant in time, owing to conservation of energy and canonical angular momentum.

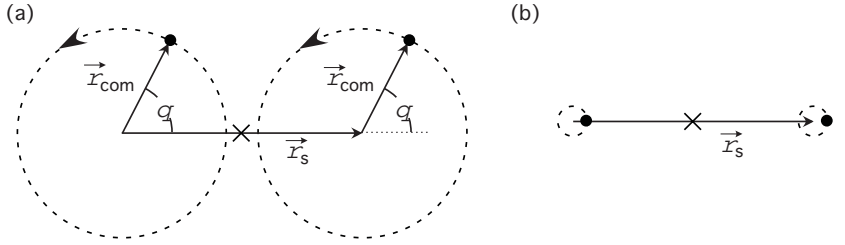

Fig. 4. Two ion magnetron mode dynamics. The magnetic field is pointing out of the plane of the figure and the center of the trap is indicated by a cross. At any time, the position of both ions can be described by the center-of-mass vector ($\boldsymbol{\rho}_{\rm com}$) and the separation vector ($\boldsymbol{\rho}_{\rm s}$). Both vectors rotate clockwise at nearly the same frequency (around 5 kHz), but the separation vector rotates about 50 mHz faster due to the Coulomb interaction between the ions (for $|\boldsymbol{\rho}_{\rm s}| \approx 1\,{\rm mm}$). So in a frame where the separation vector is stationary, the ions trace out counter-clockwise tandem circles centered on opposite sides of the center of the trap. (**a**) If $|\boldsymbol{\rho}_{\rm com}| \approx |\boldsymbol{\rho}_{\rm s}|/2$ each ion moves in and out of the center of the trap every 20 s. (**b**) If the center-of-mass mode is cooled, the ions are "parked" on nearly the same magnetron orbit. This configuration is preferable for taking cyclotron frequency data

The ideal configuration for a precise comparison of the two cyclotron frequencies is to have the two ions to go around the trap center on a common magnetron orbit of radius 500 µm, always 1 mm apart from each other. In other words, we want a magnetron difference mode amplitude of $\rho_{\rm s} \sim 1\,{\rm mm}$ and a magnetron COM mode amplitude as small as possible as shown in Fig. 4b. This configuration insures that both ions sample the same average magnetic and electrostatic fields while minimizing the ion-ion perturbations of the cyclotron frequencies. This is very important to avoid systematic errors since we know that our trapping electrostatic and magnetic fields are not perfectly homogeneous. For example, the cyclotron frequency of one ion is shifted by about 8 parts in 10^{10} between the center of the trap and a magnetron radius of 500 µm because of magnetic field inhomogeneities. In order to achieve this ideal configuration, we have developed novel techniques to precisely measure and control the individual motion of two different single ions in our Penning trap.

4.1 Two–Ion Loading Techniques

To introduce a pair of ions in the trap, we simply make the two ions one after the other using the procedure described in Sect. 3. However, since $\rho_{\rm s}$ is fixed by the separation distance between the ions when their magnetron modes couple, we must avoid making them too close to each other. Recall from Sect. 3 that our ions are created near the center of the trap, in a magnetron orbit of typically $\leq 100\,\mu{\rm m}$ radius. So the basic sequence for loading a pair is the following: we produce a single ion of the first member of our pair, say $^{13}C_2H_2^+$. We choose to make the more difficult ion to isolate first since we can then apply our cleaning techniques to remove fragments (such as $^{13}C_2H^+$, $^{13}C_2^+$, etc.). After cooling

all of the first ion's three modes of motion, we drive its magnetron radius to ∼1 mm and then make the second ion (N_2^+) near the trap center. The ion-ion separation ρ_s is then fixed to ∼1 mm and the amplitude of the magnetron COM $\rho_{com} \approx \rho_s/2 \approx 500\,\mu m$.

The motion of the two ions in this configuration is determined by the two new magnetron normal modes (COM and difference) and is illustrated in Fig. 4a. The frequency of the COM and difference modes are nearly identical (around 5 kHz) but the difference mode rotates about 50 mHz faster due to the Coulomb interaction between the ions [28]. So in a frame where the separation vector is stationary, the ions trace out counter-clockwise tandem circles centered on opposite sides of the center of the trap. This means that each ion's magnetron radius is oscillating between 0 and 1 mm every 20 seconds. The positive aspect of this "swapping motion" is that it insures that both ions experience the same average magnetic and electric fields. However, in the presence of electrostatic anharmonicities the axial frequency of an ion depends on its radial position in the trap. Since our detector relies on the narrowband nature of the ion's signal (Sect. 3.1), the less stable the axial frequency is, the more difficult it is to observe the axial motion of the ions and extract precise information from it (e.g. phase). In order to stabilize the axial frequency and reach the ideal configuration mentioned in the previous section, we need to cool the magnetron COM mode to the configuration shown in Fig. 4b.

One approach for cooling the COM motion is to apply a magnetron drive pulse with the correct amplitude and phase to drive the magnetron center-of-mass to the center of the trap. To show that we can do this, we first put a single $^{13}C_2H_2^+$ ion in the trap and drive its magnetron motion with two magnetron pulses of equal amplitude separated by a time T (analogous to the SOF technique described in Sect. 3.4). We then minimize the final magnetron amplitude by varying the relative phase between the drive pulses while holding T fixed. At the optimal phase between the drives ϕ_{min}, the ion is pulsed out to a large magnetron radius (typically 1 mm), allowed to go around its magnetron orbit at 5 kHz for T seconds, and then pulsed back to the center of the trap. We can determine ϕ_{min} with uncertainty less than one degree in about 10 min. The remaining magnetron amplitude is typically less than 100 μm. We normally use $T \approx 1$ s but we have been able to observe similar performance with T up to 10 s.

Once we know ϕ_{min}, we have what we need to introduce a pair of ions in our trap and cool their magnetron center-of-mass. We can simply use the same procedure as above with two differences: we make an N_2^+ ion near the trap center during the time T, and we make the amplitude of the second magnetron drive only half of the amplitude of the first one. Here is the sequence in details: 1) We drive $^{13}C_2H_2^+$ to a large 1 mm magnetron orbit. 2) We quickly inject N_2 gas and fire our electron beam to create one N_2^+ ion near the center of the trap. 3) T seconds after the initial magnetron pulse, we apply another magnetron drive with a phase ϕ_{min} relative to the first one and only half the amplitude. The effect of this pulse is to drive the $^{13}C_2H_2^+$ back to a radius of 500 μm, and simultaneously drives the N_2^+ out to a radius of 500 μm on the other side of the trap. The two ions should then be in the "ideal" configuration pictured in Fig. 4b.

By completely automating the ion making process we were able to execute this sequence in less than one second.

The main problem of this method is that since our electron beam is parallel to the trap axis, we often make the N_2^+ with a large axial amplitude (several mm). This greatly increases the effective distance between the two ions such that the two individual magnetron modes do not couple initially. During the several tens of seconds required to damp this axial excitation, the separation distance between the ions is not conserved and the ions are likely to end up much closer to each other than we intended. To avoid this problem we modified the method above to allow axial cooling of the N_2^+ before sending the correcting magnetron drive pulse. Just before making the N_2^+, we make the trap very anharmonic to intentionally break the degeneracy between the magnetron frequencies of the two ions (one in the center of the trap, the other in a 1 mm magnetron orbit). This allows us to cool the axial motion of the N_2^+ without worrying about the magnetron motions swapping amplitudes. However, because the cooling process takes minutes we now need to measure the phase of the $^{13}C_2H_2^+$ in order to choose the phase of our second magnetron drive. To do this, we go back to a harmonic trap and apply a short coupling pulse between the magnetron and axial modes of the $^{13}C_2H_2^+$ and extract its magnetron phase from the signal in our detector. The change in magnetron amplitude from the coupling pulse is insignificant. In principle, we could extend this technique to measure the amplitude and phase of both ions' magnetron motions and send a correction pulse to fine-tune the magnetron orbits of the ions, i.e., zero more precisely the magnetron COM mode amplitude.

Loading a pair of ions in our trap using the techniques above still requires some work, time and patience. We often have to try many times ($\sim$10) before making a pair that we can use. Most often the COM amplitude is still large and the ions are too close to each other so that the axial frequencies of the ions vary a lot very quickly (2–3 Hz in 10 s). However we are rewarded by being able to keep the same pair in the trap and perform measurements on it for many weeks.

4.2 Diagnostic Tools

By simultaneously trapping two different ions in our Penning trap, we introduce two new possible sources of systematic errors on our measurement of the cyclotron frequency ratio: (1) the Coulomb interaction between the ions and (2) the imperfection of the trapping fields away from the center of the trap. In contrast to our previous technique where we altenately trapped single ions (Sect. 3), we expect that these systematic errors will now completely dominate our final error. In order to investigate this important question, it is therefore crucial for us to be able to measure the ion-ion separation, know which part of the trap each ion samples, and precisely characterize our trapping fields. In this section, we will describe various techniques we invented to achieve this.

During the past few years, we have developed a new computer system to control our experimental setup which allows a much higher level of automation. We also accurately measured the relativistic cyclotron frequency shift versus

cyclotron radius for a single ion of Ne^{++} and Ne^{+++} and obtained from this an absolute calibration of the amplitude of our ion's motion in the trap with an accuracy of 3% [29]. This allowed us to precisely map the axial and magnetron frequency shifts of one ion in the trap as a function of absolute magnetron, cyclotron and axial amplitudes, from which we gained unprecedented knowledge of our field imperfections (electrostatic and magnetic). Using the conventions of [17] to expand the fields, we have $B_2/B_0 \approx (61 \pm 6) \times 10^{-8}/\mathrm{cm}^2$, $C_6 \approx (53 \pm 7) \times 10^{-4}$ and we can adjust C_4 to the desired value (usually zero) $\pm 1 \times 10^{-5}$ using the guard ring electrodes voltage. We also developed a computer-based feedback system to lock the axial frequency of an ion in the trap to an external frequency reference. This system now allows us to continuously monitor the axial frequency of an ion. Equipped with these new tools, we are now able to exploit the dependence of the axial frequency on magnetron radius in the presence of electrostatic anharmonicities to indirectly observe the radial position of one ion in time. This technique applied to a pair of simultaneously trapped ions allows us to experimentally observe the beat frequency between the strongly coupled magnetron modes (as each ion's magnetron radius oscillates due to a non-zero magnetron COM mode amplitude). Not only has this confirmed our model of the dynamics of two trapped ions, but it also provides us with a sensitive probe of the ion-ion separation distance. Indeed, the magnetron beat frequency scales like the inverse cube of the ion-ion separation distance. We can therefore measure where the ions are with respect to each other with a precision of a few percent and verify that their separation is constant in time at that level. This is an invaluable tool in our exploration the new systematic error on the ratio introduced by the ion-ion Coulomb force. By keeping the ions $\sim$1 mm apart, we expect the cyclotron frequency ratio to be perturbed by less than one part in 10^{11}.

We can also determine the rms magnetron radius of each ion individually by varying the size of the electrostatic anharmonicity and measuring the change in each ion's axial frequency. This is also crucial since we must know that both ions sample the same region of space to prevent magnetic field inhomogeneities from introducing a systematic error.

An unexpected effect of our axial frequency locking system is that it appears to couple our two-ion magnetron normal modes. Depending on the frequency of our cw drive relative to the axial frequency of the ion we are locking, we found that we can transfer angular momentum either from the COM mode into the difference mode or vice versa. This is a very useful tool since it allows us to completely cool the magnetron COM amplitude with the important benefits mentioned above. It also gives us the ability to change the ion-ion separation without having to load a new pair of ions in our trap. Indeed we can drive the COM magnetron mode with a dipole electric field and then use this technique to transfer that COM mode amplitude into the difference mode, thereby moving the ions further apart from each other. To reduce the ion-ion separation distance, we simply use a short axial-magnetron coupling pulse to transfer a little bit of the magnetron motion into the damped axial mode for both ions simultaneously.

4.3 Preliminary Results

Using the techniques described in the previous sections, we have been able to load the trap with two different ions species (e.g. $^{13}C_2H_2^+$ and N_2^+) and simultaneously confine them on nearly the same magnetron orbit in our Penning trap (with radius of about 500 μm). We can then apply the same techniques we used previously to measure the cyclotron frequency of a single ion in the trap (see Sect. 3), but on both ions *simultaneously*: we drive each ion's cyclotron mode to a radius of about 75 μm, let it accumulate phase for some time, and then simultaneously transfer each ion's cyclotron motion into its axial mode to read its phase. Since we have been using two ions with very similar masses ($\Delta m/m \approx 4 \times 10^{-4}$) the two axial signals are very close in frequency ($\Delta f_z \approx 50\,\mathrm{Hz}$) and they both fall within the bandwidth of our detector. The result of simultaneous cyclotron frequency comparisons is shown in Fig. 5. In these data, the shot-to-shot noise in the ratio of the cyclotron frequencies is $\sim 7 \times 10^{-11}$ after only three minutes of phase evolution – more than a factor of 10 gain in precision compared to our previous method. We have made simultaneous cyclotron frequency comparisons for periods as long 60 hours all under automated computer control and even during the daytime when magnetic field noise from the nearby subway would prevent comparisons of alternate single ions with useful precision. Unfortunately, at the time of this publication we cannot report a measured mass ratio because our study of the systematic errors associated with having both ions in the trap is still ongoing.

When measuring the cyclotron frequency ratio of CO^+/N_2^+, we have repeatedly observed abrupt and very large (∼1 part in 10^9) jumps between a few

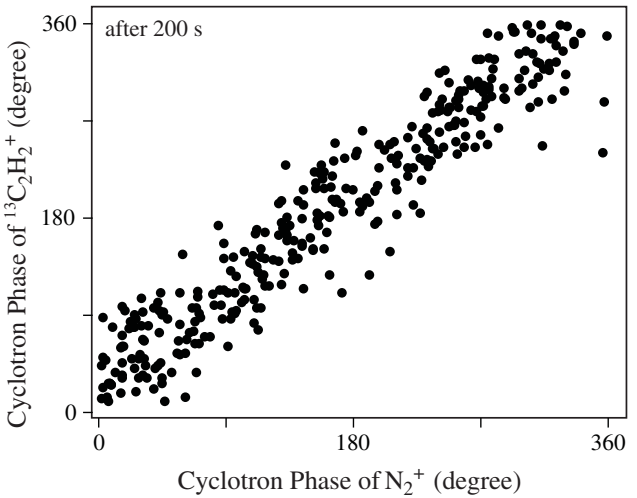

Fig. 5. Preliminary data from two different ions simultaneously confined in the same trap. Each point represents a set of cyclotron phases simultaneously accumulated in 200 s by a $^{13}C_2H_2^+$ and a N_2^+ ion plotted versus each other. The very good correlation indicates that magnetic field fluctuations are not a limitation in this technique

discrete values. No such jumps have been observed in the cyclotron frequency ratio for the experimentally very similar comparison $^{13}C_2H_2^+/N_2^+$. We currently attribute the observed jumps to black-body-induced quantum jumps among the lowest lying rotational levels of the CO^+ molecule. The cyclotron frequency is perturbed because the magnetic field orients the molecular dipole towards or away from the center of cyclotron motion depending on the molecule's rotational state. This is believed to be the first observation of the charge distribution within the molecule modifying its cyclotron frequency and might be used to determine the dipole moments of ionic molecules or for single ion molecular spectroscopy. The details of these results will be published in the next few months.

5 Subthermal Detection

For simultaneous cyclotron frequency measurements, the leading source of random error is the frequency shift associated with thermal variations in the cyclotron radius. This section will describe two techniques which we have already demonstrated to alleviate this problem.

Before every measurement, we cool the ion's motion by coupling it to our detection circuit until it comes into equilibrium with the detector. (Only the axial motion is coupled to the detector, but we cool the two radial modes using the mode coupling field mentioned in Sect. 3.2.) This remaining "4 K" motion of the ion adds vectorially to the displacement from our cyclotron drive pulses and hence prevents us from establishing an exactly reproducible amplitude and phase of motion with each excitation pulse. This effectively adds random noise to the phase we measure from one PNP sequence to the next. Since it is the same Johnson noise that drives the ion's thermal motion and is added to the ion image current to form our detected signal, these two sources of noise both contribute to our measurement error (phase noise). Moreover, the thermal cyclotron amplitude fluctuations cause relativistic mass variations and also combine with field imperfections to introduce random fluctuations of the cyclotron frequency. The cyclotron frequency variations due to special relativity is several parts in 10^{11} for $m/q \sim 20$ and close to a part in 10^{10} for lighter species such as ^{3}He and ^{3}H. After magnetic field fluctuations, this is the dominant source of noise in our alternating measurements technique, and is leading source of random error for simultaneous cyclotron frequency measurements.

5.1 Classical Squeezing

In analogy to squeezed states of light, we have demonstrated a technique in which a parametric drive at $2 \times \omega_z$ produces quadrature squeezing of the axial thermal uncertainty (Fig. 6) [30]. The squeezed thermal distribution can then be swapped into the cyclotron mode using a π-pulse. By properly adjusting the relative phase of the parametric drive and the cyclotron drive, we have demonstrated a factor of 2 reduction in the amplitude fluctuations [30]. We have also proposed two other techniques combining squeezing with selective anharmonicity that should achieve amplitude squeezing by at least a factor of 5 [31].

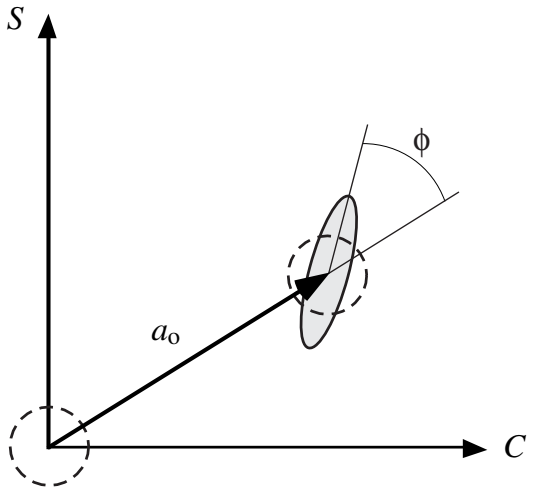

Fig. 6. Squeezing of Thermal Distribution. The finite temperature of the ion's cyclotron mode results in shot-to-shot variation of the cyclotron amplitude and phase after the initial drive pulse (indicated by a_o) of a PNP or SOF sequence. The isotropic thermal uncertainty (*dashed circle*) can be squeezed (*ellipse*) before the drive pulse to reduce either the amplitude ($\phi = 90°$) or the phase ($\phi = 0°$) uncertainty. Amplitude squeezing is more advantageous for mass measurements because amplitude fluctuations lead to shot-to-shot cyclotron frequency fluctuations due to special relativity and magnetic field inhomogeneities

5.2 Electronic Refrigeration

The other approach to address the problem of thermal variations in the cyclotron radius is to cool the detector and ion below the 4 K ambient temperature of the coupling coil and trap environment. This is done with electronic cooling [32]. This technique has the added benefit of greatly improving our signal-to-noise ratio.

The essence of electronic cooling is to measure the thermal noise in our detection transformer (referred to as the coil below), phase shift the signal and then feed it back into the detection circuit to reduces the noise currents to an effective temperature as low as 0.5 K. The key is that our dc SQUID has technical noise much lower than 4 K and can measure precisely the current in the coil in a time shorter than its thermalization time ($Q_0/\omega \sim 30$ ms). This feedback also decreases the apparent quality factor Q of the coil. Figure 7 shows the thermal noise of the coil at different gain settings of the feedback loop. Analyzing these data, we find that the thermal energy in the coil, corresponding to the area under the peak, is reduced below 4 K by the factor Q/Q_0, as expected from the detailed solution of the circuit (assuming a parallel LRC coupling coil where the resistor $R = Q_0\omega_0 L$ has the usual Johnson noise current).

With this electronic cooling technique, the ion's motion should come into equilibrium with the colder detector thereby greatly reducing the problem from amplitude fluctuations described above. Combining this with the squeezing tech-

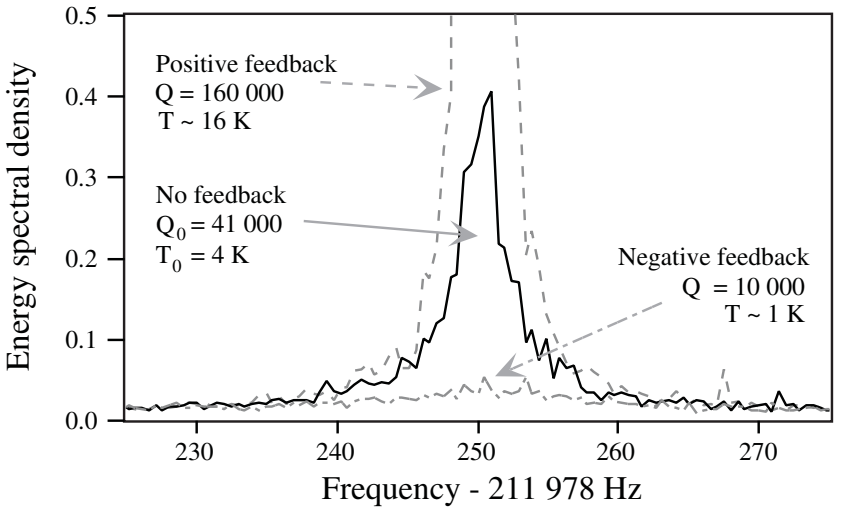

Fig. 7. Thermal profile of the detector coil as a function of the quality factor Q adjusted with the gain of the feedback. The thermal energy in the coil (area under the peak) is proportional to Q/Q_0, where Q_0 is the Q of the detector coil without feedback. This shows that the negative feedback does indeed reduce the thermal fluctuations in the coil

nique described in Sect. 5.1 should in principle reduce the shot-to-shot relativistic fluctuations of the cyclotron frequency ratio to a few parts in 10^{12} for all but the lightest species.

Another effect of the feedback is to reduce the transformer voltage across the trap which is responsible for damping the ion's axial motion. This reduces the bandwidth of our signal, increasing our signal-to-noise ratio (the Johnson noise is a constant current/$\sqrt{\text{Hz}}$). This translates directly into a better ability to estimate the parameters of the axial oscillation of the ion. With this technique, we can now measure the phase of the cyclotron motion of a single ion in the trap with an uncertainty as low as 5 degrees – more than a factor of 2 improvement. Our ability to determine the amplitude of the ion signal has also improved, again by more than a factor of 2, and we can measure the frequency of the axial motion with 4 times better precision. The better phase noise allows us to obtain the same precision on a cyclotron measurement in a shorter time. This will be important in the future since we would have to acquire data for 10 minutes to reach a precision of 10^{-11} with the previous phase noise ($\sim$ 12 degrees), or 100 minutes for 10^{-12} ! We can also use the improved signal-to-noise to reduce the cyclotron amplitude we use, which in turn reduces the frequency shifts due to relativity and field imperfections. Finally, this technique gives us the ability to arbitrarily select the damping time of the ion by changing the gain of the feedback. This opens the door for us to very high precision at small mass-to-charge ratio, (e.g. ^{6,7}Li, ^{3}He, ^{3}H) where we used to suffer from excessively short ion damping times.

6 Conclusion

To date our group has measured a total of 14 neutral masses with fractional accuracies near or below 10^{-10} with wide-ranging impact on both fundamental physics and metrology. This typically represents an improvement of two orders of magnitude in precision over the previously accepted values. This precision was achieved by comparing the cyclotron frequencies of two single atomic or molecular ions alternately confined in a Penning trap. The magnetic field fluctuations limited the precision of a given mass ratio to a few parts in 10^{-10} for a 4 hour data set during the night (when the magnetic field is quiet).

We have now successfully loaded two different single ions in the same Penning trap and demonstrated *simultaneous* measurements of their cyclotron frequencies. This technique completely eliminates the temporal variations of magnetic field as a limitation in our measurements and allows us to attain a shot-to-shot noise in the ratio of $\sim 7 \times 10^{-11}$ after only three minutes of measurement time. This represents more than a factor of 10 gain in precision compared to our previous method. We have developed novel techniques to measure and control all three normal modes of motion of each ion, including the two strongly coupled magnetron modes. These tools will be invaluable in our current investigation of the important question of systematic errors. We are hopeful that by precisely controlling the motion of the ions and characterizing the electrostatic and magnetic fields they sample, we will be able to achieve mass comparison with a resolution approaching 1×10^{-11} in the near future.

Acknowledgments

This work is supported by the National Science Foundation.

References

1. R.S. Vandyck, D.L. Farnham, and P.B. Schwinberg: Phys. Rev. Lett. **70**, 2888 (1993)
2. R. Van Dyck, D. Farnham, S. Zafonte, and P. Schwinberg: 'High precision Penning trap mass spectroscopy and a new measurement of the proton's atomic mass'. In: *International Conference on Trapped Charged Particles and Fundamental Physics, Monterey, CA, August 31–September 4, 1998,* ed. by D.H.E. Dubin, D. Schneider (AIP, Woodbury, 1998) Vol. 457, pp. 101–110
3. R.S. Van Dyck, S.L. Zafonte, and P.B. Schwinberg: Hyperfine Interact. **132**, 163 (2001)
4. F. Difilippo, V. Natarajan, K.R. Boyce, and D.E. Pritchard: Phys. Rev. Lett. **73**, 1481 (1994)
5. M.P. Bradley et al.: Phys. Rev. Lett. **83**, 4510 (1999)
6. E.R. Cohen and B.N. Taylor: Rev. Mod. Phys. **59**, 1121 (1987)
7. T. Udem et al., Phys. Rev. Lett: **79**, 2646 (1997)
8. T. Udem, J. Reichert, R. Holzwarth, and T.W. Hänsch: Phys. Rev. Lett. **82**, 3568 (1999)
9. T. Beier et al.: Phys. Rev. Lett. **88**, 011603 (2002)

10. D.L. Farnham, R.S. Vandyck, and P.B. Schwinberg: Phys. Rev. Lett. **75**, 3598 (1995)
11. S. Battesti et al.: 'Measurement of $h/M_{\rm Rb}$ with Ultracold Atoms'. In: *Conference on Precision Electromagnetic Measurements*, ed. by U. Feller (IEEE, Ottawa, Canada, 2002) p. 308
12. S. Gupta, K. Dieckmann, Z. Hadzibabic, and D.E. Pritchard: Phys. Rev. Lett. **89**, 140401 (2002)
13. E.G. Kessler et al.: Nucl. Instrum. Methods **457**, 187 (2001)
14. G.L. Greene, M.S. Dewey, E.G. Kessler, and E. Fischbach: Phys. Rev. D **44**, R2216 (1991)
15. J. Bonn et al.: Phys. Atom. Nuclei **63**, 969 (2000)
16. V.M. Lobashev: Phys. Atom. Nuclei **63**, 962 (2000)
17. L.S. Brown and G. Gabrielse: Rev. Mod. Phys. **58**, 233 (1986)
18. R.M. Weisskoff et al.: J. Appl. Phys. **63**, 4599 (1988)
19. E.A. Cornell, R.M. Weisskoff, K.R. Boyce, and D.E. Pritchard: Phys. Rev. A **41**, 312 (1990)
20. E.A. Cornell et al.: Phys. Rev. Lett. **63**, 1674 (1989)
21. V. Natarajan, K.R. Boyce, F. Difilippo, and D.E. Pritchard: Phys. Rev. Lett. **71**, 1998 (1993)
22. P. Bevington and D. Robinson: *Data Reduction and Error Analysis for the Physical Sciences*, 2nd ed. (McGraw-Hill, Boston, 1992)
23. P. Huber: *Robust Statistics* (Wiley, New York 1981)
24. P.J. Lindstrom, W.G. Mallard, Eds., *NIST Chemistry WebBook, NIST Standard Reference Database Number 69* (National Institute of Standards and Technology, Gaithersburg, 2001) (http://webbook.nist.gov)
25. G. Audi and A.H. Wapstra: Nucl. Phys. A **595**, 409 (1995)
26. A. Wapstra and G. Audi: Nuc Phys A **432**, 1 (1985)
27. E.G. Kessler et al.: Phys. Lett. A **255**, 221 (1999)
28. E.A. Cornell, K.R. Boyce, D.L.K. Fygenson, and D.E. Pritchard: Phys. Rev. A **45**, 3049 (1992)
29. S. Rainville et al.: Hyp. Interact. **132**, 177 (2001)
30. V. Natarajan, F. Difilippo, and D.E. Pritchard: Phys. Rev. Lett. **74**, 2855 (1995)
31. F. Difilippo, V. Natarajan, K.R. Boyce, and D.E. Pritchard: Phys. Rev. Lett. **68**, 2859 (1992)
32. R. Forward: J. Appl. Phys. **50**, 1 (1979)